International Journal of Mechanics and Applications 2014, 4(2): 29-49
DOI: 10.5923/j.mechanics.20140402.02

The Solution of Torsion Problem for the Bars with Irregular Cross Sections by Boundary Element Method

Hakan Türken*, **Fatma Necla Kadıoğlu, Şenol Ataoğlu**

Civil Engineering Department, Istanbul Technical University, Istanbul, Turkey

Abstract The objective of the present study is to determine the stress distribution in bars with irregular cross sections under torsion by boundary element method. For this purpose an integral equation is built via reciprocal theorem. This integral equation involves two elastostatic states for the same body. First one represents the problem to be solved while the second does a singular elastostatic state which arises due to a singular, line body force in an infinite medium. It is accepted that Saint Venant's principle is valid. The unknown of the integral equation mentioned above is the boundary value of the torsion function. In boundary element method, boundary is divided to linear elements whose end points are named as nodal points and this equation is reduced to a system of linear algebraic equations. The unknowns of this system are nodal values of torsion function. All singularities are eliminated. After evaluation torsion function, stresses can be determined inside the region. But a different formulation is necessary for determination of the unknown stress component on the boundary. By the way the torsional rigidity of the cross-section is also determined. Three sample problems are solved. In the first case cross-section is selected to be a rectangular to check the formulation. In the second sample problem a rectangular cross-section involving a notch is considered. The third sample problem is a rectangular reinforced concrete column with four rebars. For the first problem results are coincided with analytical solution. Interesting point is that the relative error has millionth order for both displacements and stresses while for torsional rigidity has .09 percent. The last problem is a mix-boundary value problem in a multiple connected region with two different materials.

Keywords Non-uniform torsion, Boundary element, Reciprocity theorem, Boundary stresses, Singular integral equation

1. Introduction

Nonuniform torsion is one of the most interested problems for scientists and engineers. Many problems are solved by different authors using different methods.

Starting point is the Saint-Venant's formulation for homogeneous bars with constant cross-sections under torsion moments acting at the ends. Formulation and analytical solutions related to simple shapes of cross-sections can be found in Muskhelishvili's book [1]. By the way, many problems are also solved by numerical methods. Finite element method is used by Ely and Zienkiewich [2] for composite bars. Jaswon and Ponter [3] applied the boundary integral method to torsion problems for different cross-sections.

Katsikadelis and Sapountzakis [4] formulated the numerical solutions of Saint-Venant's torsion problem for composite cylindrical bars of arbitrary cross-sections via boundary element method. Here, the torsion problem is reduced to a stress problem for simply connected regions. And the reciprocal identity is used for to obtain a singular integral equation whose unknown is displacement vector on the boundary of the cross-section. After this Saint-Venant's formulation is used and the boundary values of torsion function are calculated reducing the integral equation mentioned above to a system of linear algebraic equations. All singularities are eliminated. After these stress components are calculated performing the necessary derivatives of this integral equation at any point inside the boundary. This equation does not involve any singularity. But if one wants to calculate the unknown stress component on the boundary this formulation is not correct. For this purpose another formulation is obtained to eliminate the strong singularities arising during this process. In boundary element method linear elements are used. In the new formulation, the tangential stress component can be calculated on the nodal points with a single tangent. For this kind of points singularities arising in adjacent elements eliminates each other and some derivatives vanishes. Whole formulations are extended two multiple-connected regions and having two different materials. Last problem is an application two this kind of problems.

* Corresponding author:
hakanturken@gmail.com (Hakan Türken)
Published online at http://journal.sapub.org/mechanics

2. Formulation

2.1. Basic Equations

Two vector-valued functions **u(x)**, **f(x)** and a tensor valued function **τ(x)** define together an elastostatic state for a body with volume V and surface S. **u(x)**, **τ(x)** and **f(x)** represent the displacement vector, stress tensor and body force per unit volume, respectively. **x** is the position vector of any point of this region. These quantities satisfy the following equations in Cartesian coordinates.

$$\frac{\partial \tau_{ij}}{\partial x_j} + f_j = 0 \tag{1}$$

$$\tau_{ij} = \lambda \frac{\partial u_k}{\partial x_k}\delta_{ij} + \mu\left(\frac{\partial u_i}{\partial x_j} + \frac{\partial u_j}{\partial x_i}\right) \tag{2}$$

Here x_i denotes one of the Cartesian coordinates (i=1,2,3) and summation convention is valid. δ_{ij} is the Kronecker's delta, λ, μ are Lame's constants.

Let **u(x)**, **τ(x)**, **f(x)** and **u*(x)**, **τ*(x)**, **f*(x)** be two elastostatic states. The reciprocal theorem or reciprocal identitiy which is written between these two states is,

$$\int_V \mathbf{f(x)}.\mathbf{u}^*\mathbf{(x)}\,dV + \int_S \mathbf{t(x)}.\mathbf{u}^*\mathbf{(x)}\,dS$$

$$= \int_V \mathbf{f}^*\mathbf{(x)}.\mathbf{u(x)}\,dV + \int_S \mathbf{t}^*\mathbf{(x)}.\mathbf{u(x)}\,dS \tag{4}$$

Here S is boundary of volume V, **t** and $\mathbf{t}^*$ are the surface traction vectors defined as

$$\mathbf{t} = \boldsymbol{\tau}.\mathbf{n} \qquad \mathbf{t}^* = \boldsymbol{\tau}^*.\mathbf{n} \tag{5}$$

where **n** is the outward normal of the surface S.

2.2. A Singular Elastostatic State

An infinite domain having the same material with the problem to be solved is considered. Let **y** be a fixed point of this region. If a body force exists as follows:

$$f^3 = \int_{y_3=-\infty}^{+\infty} \delta(x_1-y_1)\,\delta(x_2-y_2)\,\delta(x_3-y_3)\,dy_3\,\mathbf{e_3} \tag{6}$$

$\mathbf{e_3}$ is the base vector in the x_3 direction in Cartesian coordinates. The displacement field $\mathbf{u^3}$ and stress field $\boldsymbol{\tau}^3$ related to this body force are

$$u_1^3 = u_2^3 = 0 \qquad u_3^3 = \frac{1}{2\pi\mu}\left[-\ln\rho\right] \tag{7}$$

$$\rho = \sqrt{(x_1-y_1)^2 + (x_2-y_2)^2} \tag{8}$$

$$\tau_{11}^3 = \tau_{22}^3 = \tau_{33}^3 = \tau_{12}^3 = 0 \tag{9}$$

$$\tau_{13}^3 = -\frac{1}{2\pi}\frac{x_1-y_1}{\rho^2} \qquad \tau_{23}^3 = -\frac{1}{2\pi}\frac{x_2-y_2}{\rho^2} \tag{10}$$

This formulation can be found in Banarjee and Butterfield's book [5]. Here δ(**x-y**) denotes Dirac delta function.

2.3. Nonuniform Torsion

A prismatical bar with a constant cross-section and a linear axis, under torsion is considered. x_3 axis is the axis of the bar and cross-section plane is (x_1, x_2) plane. It is a common assumption to define the components of the displacement vector due to Saint-Venant in this bar as

$$u_1 = -\omega x_3 x_2 \quad u_2 = \omega x_3 x_1 \quad u_3 = \omega\varphi(x_1, x_2) \tag{11}$$

Here ω is the relative twist and φ denotes the torsion function. φ is also an harmonic function of the variables x_1 and x_2 in the region.

Using these and constitutive equations given in (2), stress components are calculated as

$$\tau_{13} = \mu\omega\left(\frac{\partial\varphi}{\partial x_1} - x_2\right) \tag{12}$$

$$\tau_{23} = \mu\omega\left(\frac{\partial\varphi}{\partial x_2} + x_1\right) \tag{13}$$

$$\tau_{11}^3 = \tau_{22}^3 = \tau_{33}^3 = \tau_{12}^3 = 0 \tag{14}$$

Now it will be considered that the triple **u**, **τ** and **f** represent a torsion problem to be solved.

It is also an elastostatic state. Moreover it is accepted that the body force

$$\mathbf{f} = \mathbf{0} \tag{15}$$

If reciprocal identity is written between these two elastostatic state defined above

$$\int_s \mathbf{t.u^3}\,dS + \int_V \mathbf{f.u^3}\,dV = \int_s \mathbf{t^3.u}\,dS + \int_V \mathbf{f^3.u}\,dV \tag{16}$$

is obtained. Here it must be emphasized that V, S are the volume and the surface of the bar. 2c is the length of the bar and origin is selected as the centroid of the bar respectively. (e.g. Figure 1)

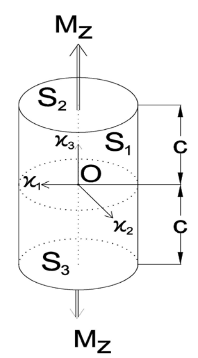

Figure 1. Prismatical bar under torsion

The surfaces S2, S3 have the same geometry. There is no surface tension on the side surface S1. τ13 and τ23 shear stresses exist on S2 and S3. This shear stresses are the same for whole cross-sections for the same x1, x2 values. Now, it will be accepted that the following line body force will be applied to any y(y1,y2) point as

$$\mathbf{f^3} = \int_{y_3=-\infty}^{+\infty} \delta(x_1-y_1)\,\delta(x_2-y_2)\,\delta(x_3-y_3)\,dy_3\,\mathbf{e_3}$$

$$= \delta(x_1-y_1)\,\delta(x_2-y_2)\mathbf{e_3} \tag{17}$$

Because of (15) the second integral in (16) is vanish. The last integral in (16) can be calculated as follow:

$$\int_V \mathbf{f^3}.\mathbf{u}\,dV =$$

$$\int_{x_3=-c}^{+c} dx_3 \int_{S_2} \delta(x_1-y_1)\,\delta(x_2-y_2)\,u_3(x_1,x_2)\,dx_1 dx_2$$

$$= u_3(y_1,y_2)2c \tag{18}$$

Substituting (18) in (16)

$$u_3(y_1,y_2)2c = \int_s \mathbf{t}.\mathbf{u}^3\,dS - \int_s \overset{3}{\mathbf{t}}.\mathbf{u}\,dS \tag{19}$$

is found. Here S is the total surface of the bar and it can be partitioned as follow:

$$S = S_1 + S_2 + S_3 \tag{20}$$

meanwhile (19) can be written as

$$u_3(y_1,y_2)2c = \int_{s_1} \mathbf{t}.\mathbf{u}^3\,dS_1 + \int_{s_2} \mathbf{t}.\mathbf{u}^3\,dS_2 + \int_{s_3} \mathbf{t}.\mathbf{u}^3\,dS_3$$

$$-\int_{s_1} \overset{3}{\mathbf{t}}.\mathbf{u}\,dS_1 - \int_{s_2} \overset{3}{\mathbf{t}}.\mathbf{u}\,dS_2 - \int_{s_3} \overset{3}{\mathbf{t}}.\mathbf{u}\,dS_3 \tag{21}$$

The first integral in (21) is vanish since S_1 is stress-free. The second and third integrals are also vanish since **t** has only components in x_1 and x_2 directions and $\mathbf{u^3}$ has only third component on S_2 and S_3 surfaces. Again considering the stresses and the normals the fourth integral is:

$$-\int_{s_1} \overset{3}{\mathbf{t}}(S_1).\mathbf{u}\,dS_1 = -2c\oint_C (\overset{3}{\tau}_{13}n_1 + \overset{3}{\tau}_{23}n_2)\,u_3(x_1,x_2)\,dC \tag{22}$$

Here C is the closed contour of S_1. If (11) is considered the last two equations of (21) become

$$\int_{s_2} \overset{3}{\mathbf{t}}.\mathbf{u}\,dS_2 - \int_{s_3} \overset{3}{\mathbf{t}}.\mathbf{u}\,dS_3 = 2\omega c \int_{S_2} \left[\overset{3}{\tau}_{13}x_2 + \overset{3}{\tau}_{23}x_1\right] dS_2 \tag{23}$$

Substitution (10) in (23) and inverting surface integral to a contour integral gives

$$2\omega c \int_{S_2} \left[\overset{3}{\tau}_{13}x_2 + \overset{3}{\tau}_{23}x_1\right] dS_2$$

$$= \frac{-2\omega c}{2\pi} \int_{S_2} \left[\frac{(x_1-y_1)\,x_2-(x_2-y_2)\,x_1}{\rho^2}\right] dS_2$$

$$= \frac{-2\omega c}{2\pi} \int_C \left(x_2 n_1 \ln\rho - x_1 n_2 \ln\rho\right) dC \tag{24}$$

The first three integrals in (21) have been eliminated and fourth integral has been calculated in (22). Remaining two integrals are also given in (24). Substituting (24) and (22) in (21), inverting u_3 to $\omega\varphi$ and using (10) leads (21) to the following integral equation.

$$\begin{matrix} \varphi(y) & (y \in S_1) \\ 0 & (y \notin S_1) \end{matrix} =$$

$$\oint_C \frac{1}{2\pi}\varphi(x_1,x_2)\left[\frac{(x_1-y_1)\,n_1-(x_2-y_2)\,n_2}{\rho^2}\right] dC$$

$$-\frac{1}{2\pi}\int_C \left(x_2 n_1 \ln\rho - x_1 n_2 \ln\rho\right) dC \tag{25}$$

The unknown of this integral equation is φ function and this formula is valid for simply-connected regions.

2.4. BEM Formulation

It is clear that if the boundary values of φ are known any value of φ inside the region can be calculated using the expression (25) given above. Then the problem is reduced to the determination of boundary values of φ function. To solve this problem boundary of the cross-section is considered as a collection of linear segments which are named as boundary elements. Besides, end points of these linear elements are named as nodal points.

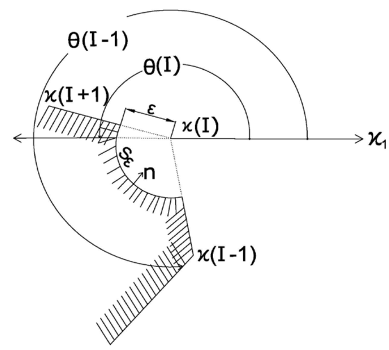

Figure 2. Artificial boundary

Linear elements are named as the same with starting points of the elements. Here on any J'th linear element the variation of φ function has been accepted as follow:

$$\varphi(\mathrm{x}) = \varphi(\mathrm{J}) + \frac{\varphi(\mathrm{J}+1) - \varphi(\mathrm{J})}{\mathrm{l}(\mathrm{J})}\mathrm{s} \tag{26}$$

Here l(J) is the length of the element and s is the distance to starting point of the (J)'th element. Substitution of (26) in (25) reduces unknowns of the problem to the nodal values of the φ function. To determine the boundary or nodal values of φ a new artificial boundary is defined for any **x(I)** nodal point which is given by Kadioglu N, Ataoglu S. [6] (e.g Figure 2) Here a circular arc Sε centred at **x(I)** with radius ε is added to the boundary so that, **x(I)** point is outside the region. Suppose the number of the nodal point is N. Then the number of the unknowns is also N and N equation is necessary. The loading point **y** is selected as any nodal point **x(I)** and calculating necessary integrals an equation is obtained. Repeating the same process for whole nodal points N equation is obtained. If the artificial boundary is used, **x(I)** point is outside of the region. Then the left side of (25) is equal to zero. Some integrals related to elements (I-1)'th and I'th, involve singularities. It is also accepted that displacement component u_3 or φ is constant on the circular arc Sε and necessary integrals are also calculated on this circular arc. After these ε will be taken as zero. Before this limit new form of (25) is below

$$0 = \sum_{\mathrm{J}=2}^{\mathrm{N}+2} \int_{\mathrm{l(J)}} \left[\phi(\mathrm{J}) + \frac{\phi(\mathrm{J}+1) - \phi(\mathrm{J})}{\mathrm{l(J)}}\right]$$
$$\left[\frac{(\mathrm{x}_1 - \mathrm{x}_1(\mathrm{I}))\mathrm{n}_1(\mathrm{J}) - (\mathrm{x}_2 - \mathrm{x}_2(\mathrm{I}))\mathrm{n}_2(\mathrm{J})}{\rho^2}\right]\mathrm{ds}$$
$$-\frac{1}{2\pi}\sum_{\mathrm{J}=2}^{\mathrm{N}+1}\int_{\mathrm{l(J)}} \ln\rho\big(\mathrm{x}_2\mathrm{n}_1(\mathrm{J}) - \mathrm{x}_1\mathrm{n}_2(\mathrm{J})\big)\mathrm{ds}$$
$$+\frac{1}{2\pi}\int_{\mathrm{S}\varepsilon}\left[\frac{(\mathrm{x}_1 - \mathrm{x}_1(\mathrm{I}))\mathrm{n}_1 - (\mathrm{x}_2 - \mathrm{x}_2(\mathrm{I}))\mathrm{n}_2}{\rho^2}\right]\phi(\mathrm{I})\,\mathrm{dS}\varepsilon$$
$$-\frac{1}{2\pi}\int_{\mathrm{S}\varepsilon}\ln\rho\big(\mathrm{x}_2\mathrm{n}_1 - \mathrm{x}_1\mathrm{n}_2\big)\mathrm{dS}\varepsilon \tag{27}$$

Numbering starts from 2 and the last nodal point is (N+1)'th. The nodal point having number 1 coincides with (N+1)'th and 2 coincides with (N+2)'th. (27) can be simplified as follows by calculating necessary integrals.

$$(\mathrm{I} = 2, \mathrm{N}+1)$$

$$\sum_{\mathrm{J}=2}^{\mathrm{N}+2}\left[\phi(\mathrm{J})\,\mathrm{W1(I,J)} + (\phi(\mathrm{J}+1) - \phi(\mathrm{J}))\,\mathrm{T(I,J)}\right]$$
$$+\sum_{\mathrm{J}=2}^{\mathrm{N}+2}\mathrm{W2(I,J)} + \phi(\mathrm{I})\,\mathrm{E1(I)} + \mathrm{E2(I)} = 0 \tag{28}$$

Abbreviations W1(I,J), W2(I,J), E1(I,J), E2(I,J), T(I,J) in (28) are given as follows:

$$(\mathrm{J} \neq \mathrm{I}, \mathrm{I}-1)$$

$$\mathrm{W1(I,J)} = \int_{l(J)}\left[\frac{(\mathrm{x}_1 - \mathrm{x}_1(\mathrm{I}))\mathrm{n}_1(\mathrm{J}) + (\mathrm{x}_2 - \mathrm{x}_2(\mathrm{I}))\mathrm{n}_2(\mathrm{J})}{\rho^2}\right]\mathrm{ds} \tag{29}$$

$$(\mathrm{J} \neq \mathrm{I}, \mathrm{I}-1)$$

$$T(\mathrm{I,J}) = \int_{l(J)}\left[\frac{(\mathrm{x}_1 - \mathrm{x}_1(\mathrm{I}))\mathrm{n}_1(\mathrm{J}) + (\mathrm{x}_2 - \mathrm{x}_2(\mathrm{I}))\mathrm{n}_2(\mathrm{J})}{\rho^2}\right]\frac{s}{l(J)}\mathrm{ds} \tag{30}$$

$$(\mathrm{J} \neq \mathrm{I}, \mathrm{I}-1)$$

$$\mathrm{W2(I,J)} = -\frac{1}{2\pi}\int_{\mathrm{l(J)}}\ln\rho\big(\mathrm{x}_2\mathrm{n}_1(\mathrm{J}) - \mathrm{x}_1\mathrm{n}_2(\mathrm{J})\big)\mathrm{ds} \tag{31}$$

$$E1(\mathrm{I}) = \lim_{\varepsilon\to 0}\frac{1}{2\pi}\int_{\mathrm{S}\varepsilon}\frac{(\mathrm{x}_1 - \mathrm{x}_1(\mathrm{I}))\mathrm{n}_1 + (\mathrm{x}_2 - \mathrm{x}_2(\mathrm{I}))\mathrm{n}_2}{\rho^2}\mathrm{dS}\varepsilon \tag{32}$$

$$E2(\mathrm{I}) = -\frac{1}{2\pi}\lim_{\varepsilon\to 0}\int_{S\varepsilon}\ln\rho\big(\mathrm{x}_2\mathrm{n}_1 - \mathrm{x}_1\mathrm{n}_2\big)\,\mathrm{d}S\varepsilon \tag{33}$$

This integrals have been calculated analytically and have been given in Appendix I except E1(I) and E2(I) which are given below:

$$\mathrm{E1(I)} = \frac{1}{2\pi}\int_{\theta=\theta(\mathrm{I}-1)}^{\theta(\mathrm{I})}\mathrm{d}\theta = \frac{1}{2\pi}\big[\theta(\mathrm{I}) - \theta(\mathrm{I}-1)\big] \tag{34}$$

$$\mathrm{E2(I)} = 0 \tag{35}$$

The angles Θ(I) and Θ(I-1) are given in Figure 2. And some special cases for J=I and J=I-1 related to other integrals are

$$\mathrm{W1(I,I-1)} = 0 \tag{36}$$

$$\mathrm{T(I,I-1)} = 0 \tag{37}$$

$$\mathrm{W2(I,I-1)} = -\frac{1}{2\pi}\Bigg[-\frac{\mathrm{l(I-1)}^2}{4}(2\ln\mathrm{l(I-1)} - 1)$$
$$+\big[\mathrm{l(I-1)} + \mathrm{x}_2(\mathrm{I}-1)\mathrm{n}_1(\mathrm{I}-1) - \mathrm{x}_1(\mathrm{I}-1)\mathrm{n}_2(\mathrm{I}-1)\big]$$
$$l(I-1)\big[\ln(I-1) - 1\big]\Bigg] \tag{38}$$

$$\mathrm{W1(I,I)} = 0 \tag{39}$$

$$T(\mathrm{I,I}) = 0 \tag{40}$$

$$\mathrm{W2(I,I)} = -\frac{1}{2\pi}\Bigg[\frac{\mathrm{l(I)}^2}{4}\big[2\ln\mathrm{l(I)} - 1\big]\big[\mathrm{n}_1\mathrm{x}_2(\mathrm{I}) - \mathrm{n}_2\mathrm{x}_1(\mathrm{I})\big]$$
$$l(I)\ln l(I) - l(I)\Bigg] \tag{41}$$

(28) defines a system of linear algebraic equations as follows:

$$\mathbf{AX} = \mathbf{K} \tag{42}$$

Here **A** is a matrix of order N × N, **X** and **K** are matrices of order N × 1, any element of these can be defined as

For (I,J)=1,…,N

$$A(I,J) = W1(I+1,J+1) - T(I+1,J+1)$$
$$+ \mathrm{T}(\mathrm{I}+1,\mathrm{J}) + \delta_{\mathrm{IJ}}\mathrm{E1}(\mathrm{I}) \tag{43}$$

$$\mathrm{K(I)} = -\sum_{\mathrm{J}=1}^{\mathrm{N}} \mathrm{W2(I+1,J+1)} \tag{44}$$

$$\mathrm{X(I)} = \varphi(\mathrm{I}+1) \tag{45}$$

Here δ_{IJ} is Kronecker's delta.

Solution of this system of linear equations gives the nodal values of φ function. After finding these values using (25) φ(**y**) value for any **y** inside the region can be calculated and this calculation does not involve any singularity and the exact solutions of the integrals given in Appendix can be used neglecting E1. For any **y** inside the region this equation is

$$\sum_{\mathrm{J}=2}^{\mathrm{N}+1}\left[\phi(\mathrm{J})\,\mathrm{W1}(\mathbf{y},\mathrm{J}) + (\phi(\mathrm{J}+1-\phi(\mathrm{J}))\,\mathrm{T}(\mathbf{y},\mathrm{J})\right]$$

$$\sum_{J=2}^{N+1} W2(\mathbf{y},J) = \phi(\mathbf{y}(y_1,y_2)) \tag{46}$$

One must remember that in the expressions in (46) the coordinates of **y** point are used as the coordinates of loading point.

After these stress components can be easily calculated by taking necessary derivatives of (46) and using (12), (13) as follows. But it must be emphasized that **y** is not a boundary point.

$$\frac{\tau_{13}(\mathbf{y})}{\omega\mu} = \sum_{\mathrm{J}=2}^{\mathrm{N}+1}\left[\phi(\mathrm{J})\frac{\mathrm{W1}(\mathbf{y},\mathrm{J})}{\partial \mathrm{y}_1} + (\phi(\mathrm{J}+1)-\phi(\mathrm{J}))\right]\frac{\partial \mathrm{T}(\mathbf{y},\mathrm{J})}{\partial \mathrm{y}_1}$$
$$+\sum_{J=2}^{N+1}\frac{\partial W2(\mathbf{y},J)}{\partial y_1} - y_2 \tag{47}$$

$$\frac{\tau_{23}(\mathbf{y})}{\omega\mu} = \sum_{\mathrm{J}=2}^{\mathrm{N}+1}\left[\phi(\mathrm{J})\frac{\mathrm{W1}(\mathrm{y},\mathrm{J})}{\partial \mathrm{y}_2} + (\phi(\mathrm{J}+1)-\phi(\mathrm{J}))\right]\frac{\partial \mathrm{T}(\mathrm{y},\mathrm{J})}{\partial \mathrm{y}_2}$$
$$+\sum_{J=2}^{N+1}\frac{\partial W2(\mathbf{y},J)}{\partial y_2} + y_1 \tag{48}$$

The expressions of W1(**y**,J), T(**y**,J) and W2(**y**,J) can be found in Appendix setting $x_1(I)=y_1$ and $x_2(I)=y_2$. And the necessary derivatives can be calculated analytically using these expressions. After these the torsional rigidity of the cross-section will be calculated. For this purpose at first the torsion moment acting on the cross-section must be calculated. It is known that torsion moment M_Z is the resultant of shear stresses acting on the cross-section. If this is written as follow:

$$\mathrm{M_Z} = \omega\mu\int_{\mathrm{S}_1}(-\tau_{13}\mathrm{x}_2 + \tau_{23}\mathrm{x}_1)\,\mathrm{dS}_1 \tag{49}$$

is found. If the expressions of the shear stresses given in (12) and (13) are used in (49).

$$\mathrm{M_Z} = \mu\omega\int_{\mathrm{S}_1}\left[-\mathrm{x}_2\frac{\partial\phi}{\partial \mathrm{x}_1} + \mathrm{x}_1\frac{\partial\phi}{\partial \mathrm{x}_2} + \mathrm{x}_1^2 + \mathrm{x}_2^2\right]\mathrm{dS}_1 \tag{50}$$

is found. Expression (50) can be transformed to a contour integral as below:

$$\mathrm{M_Z} = \mu\omega\int_{\mathrm{S}_1}\left[\frac{\partial}{\partial \mathrm{x}_1}(-\phi\,\mathrm{x}_2) + \frac{\partial}{\partial \mathrm{x}_2}(\phi\,\mathrm{x}_1)\right.$$
$$\left.+\frac{\partial}{\partial \mathrm{x}_1}\left(\frac{\mathrm{x}_1^3}{3}\right) + \frac{\partial}{\partial \mathrm{x}_2}\left(\frac{\mathrm{x}_2^3}{3}\right)\right]\mathrm{dS}_1 \tag{51}$$

$$\mathrm{M_Z} = \mu\omega\oint_{\mathrm{C}}\left[(-\varphi\,\mathrm{x}_2\mathrm{n}_1 + \varphi\,\mathrm{x}_1\mathrm{n}_2)\right.$$
$$\left.+\left(\frac{\mathrm{x}_1^3\mathrm{n}_1}{3} + \frac{\mathrm{x}_2^3\mathrm{n}_2}{3}\right)\right]\mathrm{dC} \tag{52}$$

If the decomposition of the C contour to line elements and the variation of φ(s) function on these elements are considered (52) transform to the following form.

$$\mathrm{M_Z} = \mu\omega\left[\sum_{\mathrm{J}=2}^{\mathrm{N}+1}\int_{\mathrm{l(J)}}\left[\phi(\mathrm{J}) + \frac{\phi(\mathrm{J}+1)-\phi(\mathrm{J})}{\mathrm{l(J)}}\mathrm{s}\right]\right.$$
$$\left.(\mathrm{x}_1\mathrm{n}_2 - \mathrm{x}_2\mathrm{n}_1)\,\mathrm{ds} + \sum_{\mathrm{J}=2}^{\mathrm{N}+1}\int_{\mathrm{l(J)}}\frac{\mathrm{x}_1^3\mathrm{n}_1 + \mathrm{x}_2^3\mathrm{n}_2}{3}\,\mathrm{ds}\right] \tag{53}$$

Considering the definition of torsional rigidity D as:

$$D = \frac{\mathrm{M_Z}}{\omega} \tag{54}$$

$$\mathrm{R} = \frac{D}{\mu} = \left[\sum_{\mathrm{J}=2}^{\mathrm{N}+1}\int_{\mathrm{l(J)}}\left[\phi(\mathrm{J}) + \frac{\phi(\mathrm{J}+1)-\phi(\mathrm{J})}{\mathrm{l(J)}}\mathrm{s}\right](\mathrm{x}_1\mathrm{n}_2 - \mathrm{x}_2\mathrm{n}_1)\,\mathrm{ds}\right.$$

$$+\sum_{J=2}^{N+1}\int_{l(J)}\frac{x_1^3 n_1+x_2^3 n_2}{3}ds\Bigg] \tag{55}$$

is obtained. Integrals given in equation above have been calculated analytically.

If one wants to calculate the stress components on a nodal point (47) and (48) cannot be used since they involve strong singularities. If **y** is a nodal point **x(I)** these singularities cannot be eliminated in these equations. To overcome this problem, at first one must remember that the stress component on the boundary is zero. The nonzero component on the boundary is

$$\tau_s = -n_2(I)\tau_{13}(I)+n_1(I)\tau_{23}(I) \tag{56}$$

There are some restrictions to calculate $\tau_s(I)$ stress component. At first the boundary which is the sum of the line elements, will be considered as the boundary. Besides the formulation allows to calculate the stress component at a point with a single tangent, only. This means any calculation cannot be performed at the corners in the formulation given here. In addition to these the necessary derivatives which will be used in the expressions of τ_{13} **(x(I))** and τ_{23}**(x(I))** cannot be performed using (46). Now a new artificial boundary will be defined (e.g. Figure 3)

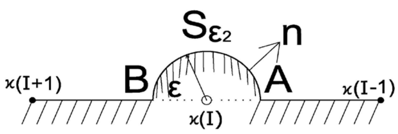

Figure 3. New artificial boundary

In this new boundary **y=x(I)** point is an inner point but (46) takes the following form calculating some integrals over the elements having **y** as an end point:

$$\phi(I)=\sum_{J=2}^{I-2}\left[\phi(J)\,W1(I,J)+(\phi(J+1)-\phi(J))\,T(I,J)\right]$$

$$+\sum_{J=I+1}^{N+1}\left[\phi(J)\,W1(I,J)+(\phi(J+1)-\phi(J))\,T(I,J)\right]$$

$$KAT1(I)\varphi(I-1)+KAT2(I)\varphi(I)+KAT3(I)\varphi(I+1)$$

$$+\sum_{J=2}^{I-2}W2(I,J)+\sum_{J=I+1}^{N+1}W2(I,J)+KAT4(I) \tag{57}$$

The abreviations in (57) are given as follows:

$$KAT1(I)=0 \tag{58}$$

$$KAT2(I)=0 \tag{59}$$

$$KAT3(I)=0 \tag{60}$$

$$KAT4(I)=-\frac{1}{2\pi}\int_{l(I-1)}\ln\rho\,(x_2n_1-x_1n_2)\,ds$$

$$-\frac{1}{2\pi}\int_{l(I)}\ln\rho\,(x_2n_1-x_1n_2)\,ds \tag{61}$$

Substituting (58), (59) and (60) in (57) the expression of φ(y) is obtained as follows:

$$\frac{1}{2}\phi(I)=\sum_{J=2}^{I-2}\left[\phi(J)\,W1(I,J)+(\phi(J+1)-\phi(J))\,T(I,J)\right]$$

$$+\sum_{J=I+1}^{N+1}\left[\phi(J)\,W1(I,J)+(\phi(J+1)-\phi(J))\,T(I,J)\right]$$

$$+\sum_{J=2}^{I-2}W2(I,J)+\sum_{J=I+1}^{N+1}W2(I,J)+KAT4(I) \tag{62}$$

This equation is proper for calculating necessary derivatives which arising in the expressions of τ_{13}(**y**) and τ_{23}(**y**)

The expressions of W1(I,J), W2(I,J) and T(I,J) have been given in Appendix. Then performing derivatives

$$\frac{\tau_{13}(\mathbf{y})}{\omega\mu}=2\left[\sum_{J=2}^{I-2}\left[\phi(J)\frac{\partial W1(I,J)}{\partial y_1}+(\phi(J+1)-\phi(J))\frac{\partial T(I,J)}{\partial y_1}\right]\right.$$

$$+\sum_{J=I+1}^{N+1}\left[\phi(J)\frac{\partial W1(I,J)}{\partial y_1}+(\phi(J+1)-\phi(J))\frac{\partial T(I,J)}{\partial y_1}\right]$$

$$\left.+\sum_{J=2}^{I-2}\frac{\partial W2(I,J)}{\partial y_1}+\sum_{J=I+1}^{N+1}\frac{\partial W2(I,J)}{\partial y_1}+\frac{\partial KAT4(I)}{\partial y_1}-y_2\right] \tag{63}$$

$$\frac{\tau_{23}(\mathbf{y})}{\omega\mu}=2\left[\sum_{J=2}^{I-2}\left[\phi(J)\frac{\partial W1(I,J)}{\partial y_2}+(\phi(J+1)-\phi(J))\frac{\partial T(I,J)}{\partial y_2}\right]\right.$$

$$+\sum_{J=I+1}^{N+1}\left[\phi(J)\frac{\partial W1(I,J)}{\partial y_2}+(\phi(J+1)-\phi(J))\frac{\partial T(I,J)}{\partial y_2}\right]$$

$$\left.+\sum_{J=2}^{I-2}\frac{\partial W2(I,J)}{\partial y_2}+\sum_{J=I+1}^{N+1}\frac{\partial W2(I,J)}{\partial y_{21}}+\frac{\partial KAT4(I)}{\partial y_2}+y_1\right] \tag{64}$$

is obtained. In these integrals, the derivatives of KAT4(I) involve singularities but substitution of (63) and (64) in (56) eliminates these singular terms. Then unknown stress component τ_s(y) is calculated for any **y=x(I)** nodal point.

3. Sample Problem

For numerical results first selected problem is a rectangular cross-section with width b=60cm and length h=100cm (e.g. Figure 4).

Second sample problem is the same rectangular but having a triangular notch. (e.g. Figure 5).

For the first problem variation of φ function versus x_2 on BC line is given in Figure 6. The variation of φ versus x_1 on EC given in Figure 7. The results given by Muskhelishvili for the same problem are also given in this figures. A table is also added to this figure since differences are very small. Practically relative error is zero for φ function.

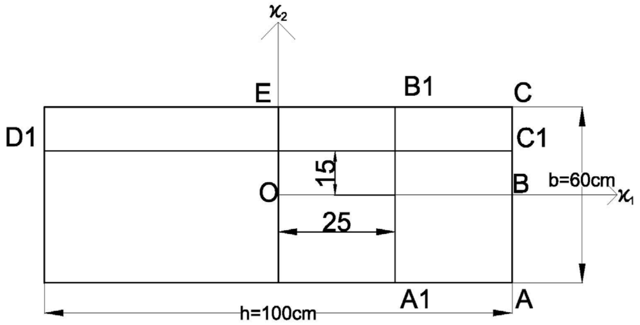

Figure 4. Rectangular cross-section

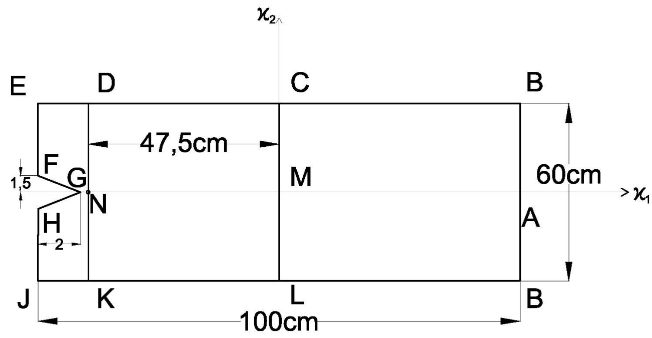

Figure 5. Rectangular cross-section with a triangular notch

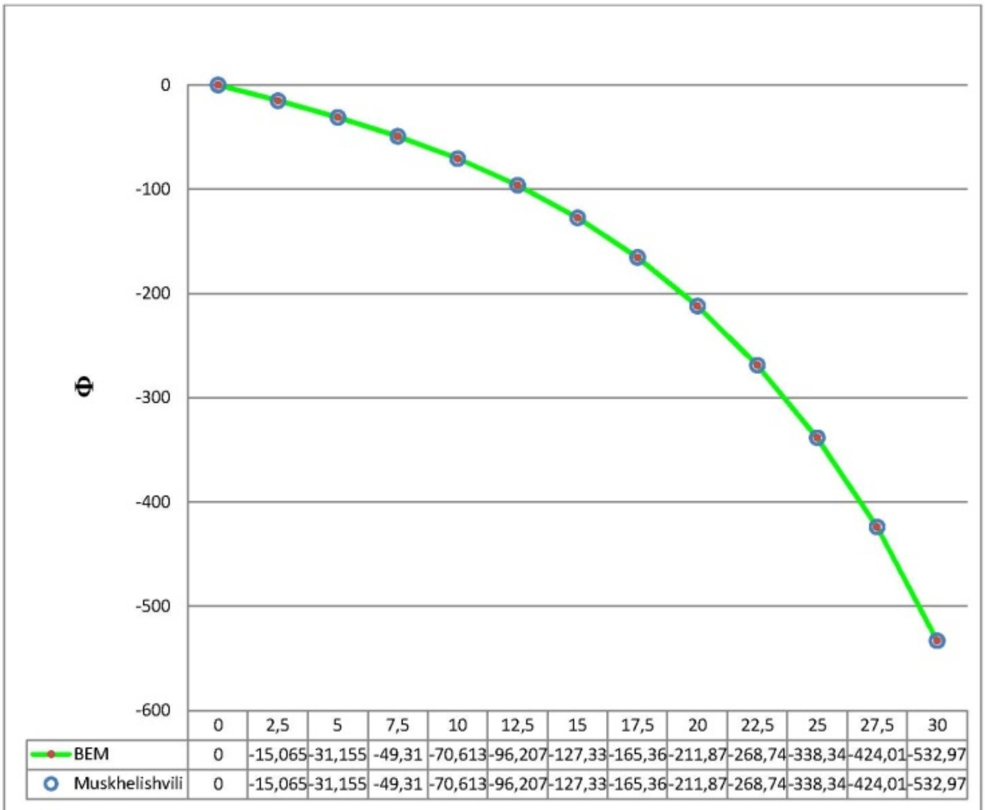

	0	2,5	5	7,5	10	12,5	15	17,5	20	22,5	25	27,5	30
BEM	0	-15,065	-31,155	-49,31	-70,613	-96,207	-127,33	-165,36	-211,87	-268,74	-338,34	-424,01	-532,97
Muskhelishvili	0	-15,065	-31,155	-49,31	-70,613	-96,207	-127,33	-165,36	-211,87	-268,74	-338,34	-424,01	-532,97

Figure 6. Variation of φ versus x_2 on BC line in rectangular

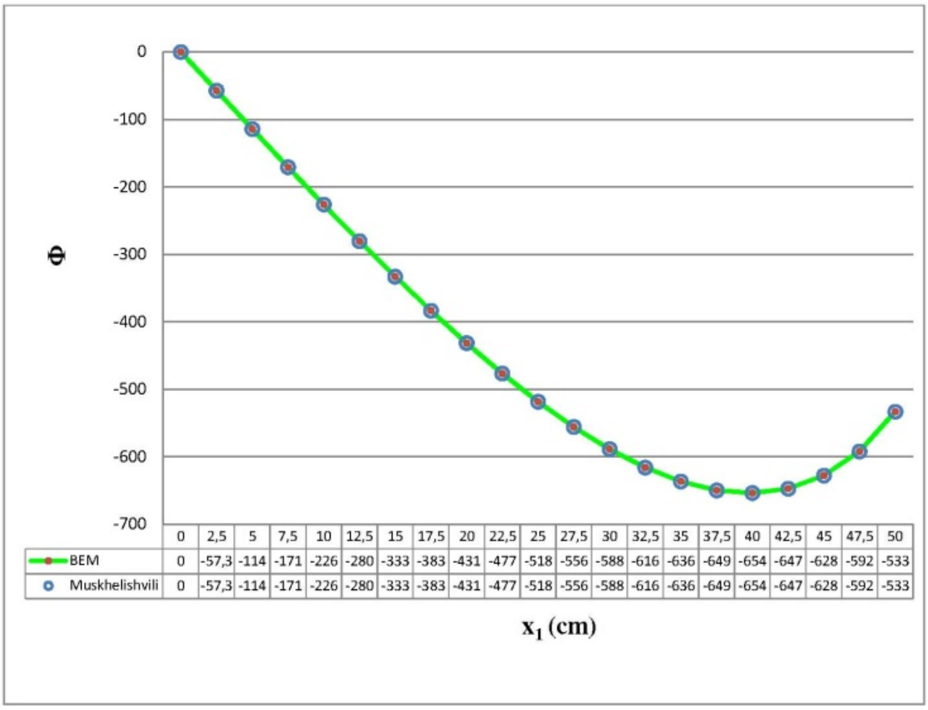

Figure 7. Variation of φ versus x_1 on EC line in rectangular

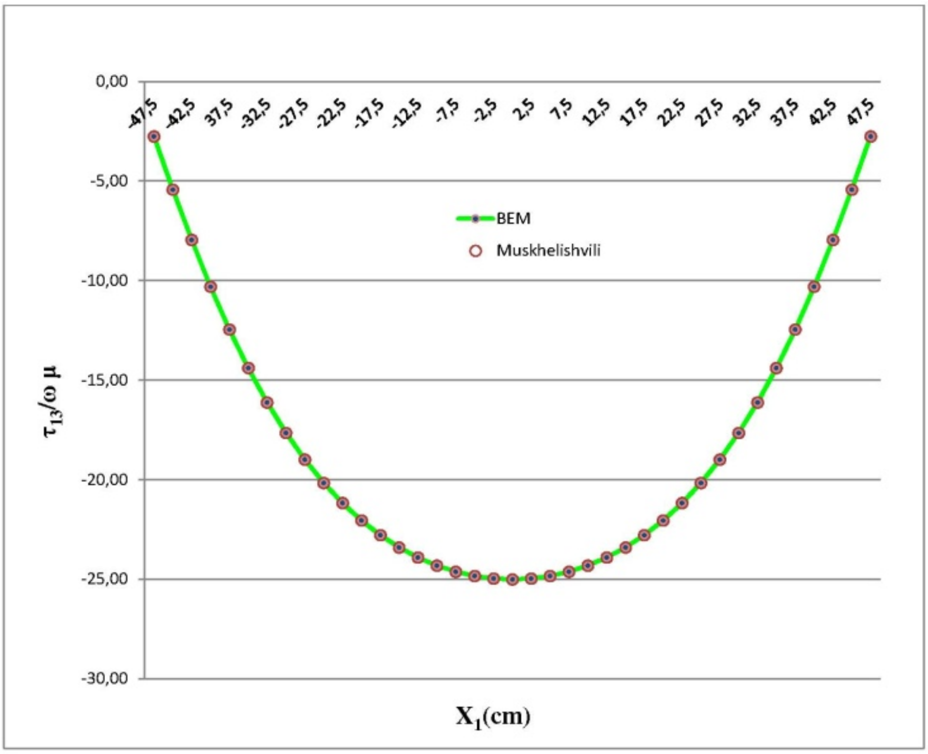

Figure 8. Variation of $\tau_{13}/\omega\mu$ versus x_1 on D1C1 line in rectangular

The variation of τ_{13} versus x_1 on D1C1 line is given in Figure 8. The variation of τ_{23} versus x_1 on the same line is given in Figure 9. The variation of τ_{13} versus x_2 on A1B1 line is given in Figure 10. The variation of τ_{23} versus x_2 on the same line is given in Figure 11. Relative error practically is also zero for shear stresses. Division of torsional rigidity to μ_1 equal R is calculated for the selected rectangular cross-section, numerical result and Muskhelishvili's result are given as follows:

$$\mathrm{R(Muskhelishvili)} = 4505976\,\mathrm{cm}^4$$

$$\mathrm{R}(BEM) = 4510142\,\mathrm{cm}^4$$

Relative error is 0.00092 for R. For the same problem variation of τ_s versus x_2 is given in Figure 12 on BC boundary and variation of τ_s versus x_1 on EC boundary is given in Figure 13. The relative error has millionth order which is practically zero.

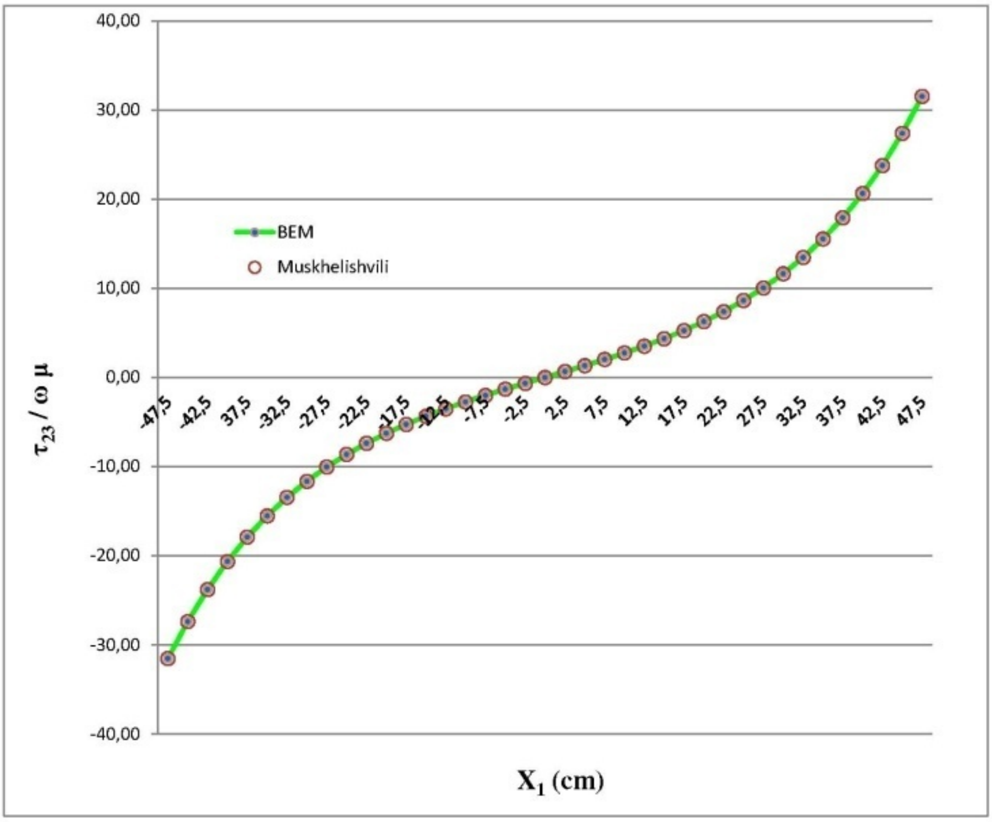

Figure 9. Variation of $\tau_{23}/\omega\mu$ versus x_1 on D1C1 line in rectangular

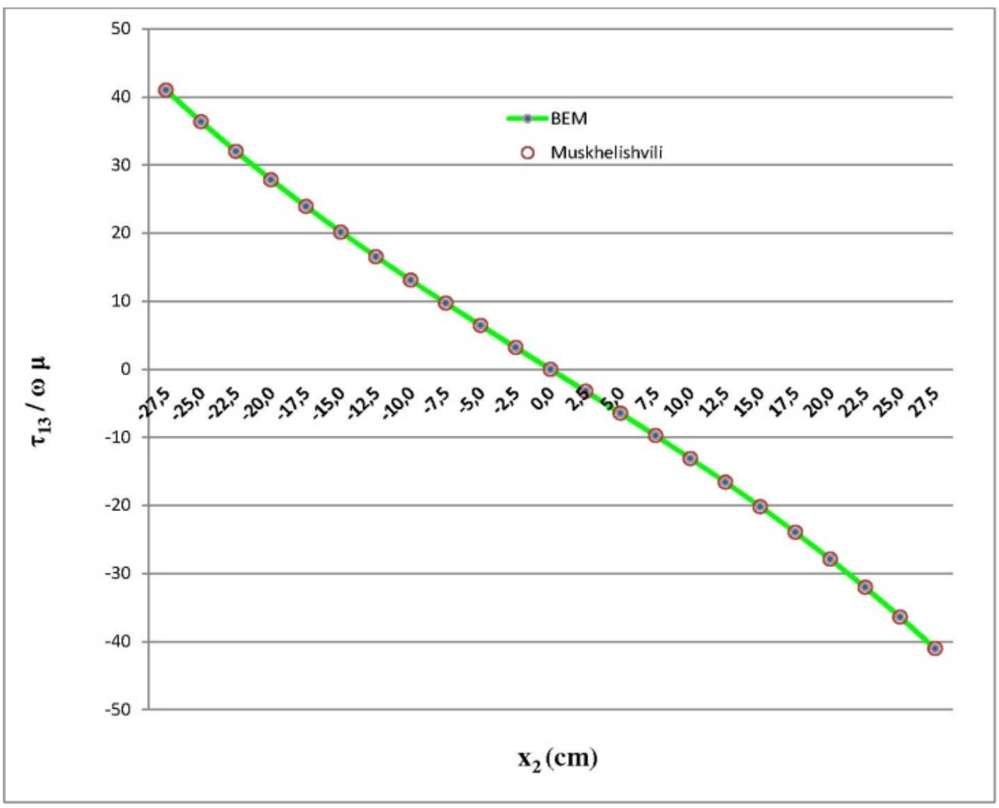

Figure 10. Variation of $\tau_{13}/\omega\mu$ versus x_2 on A1B1 line in rectangular

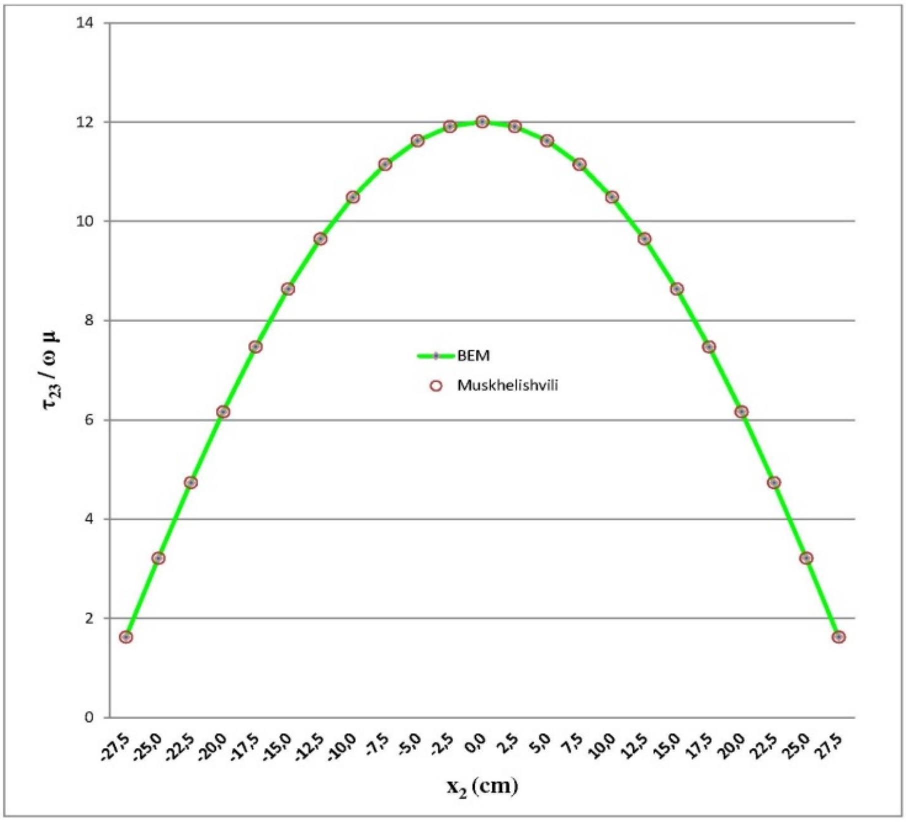

Figure 11. Variation of $\tau_{23}/\omega\mu$ versus x_2 on A1B1 line in rectangular

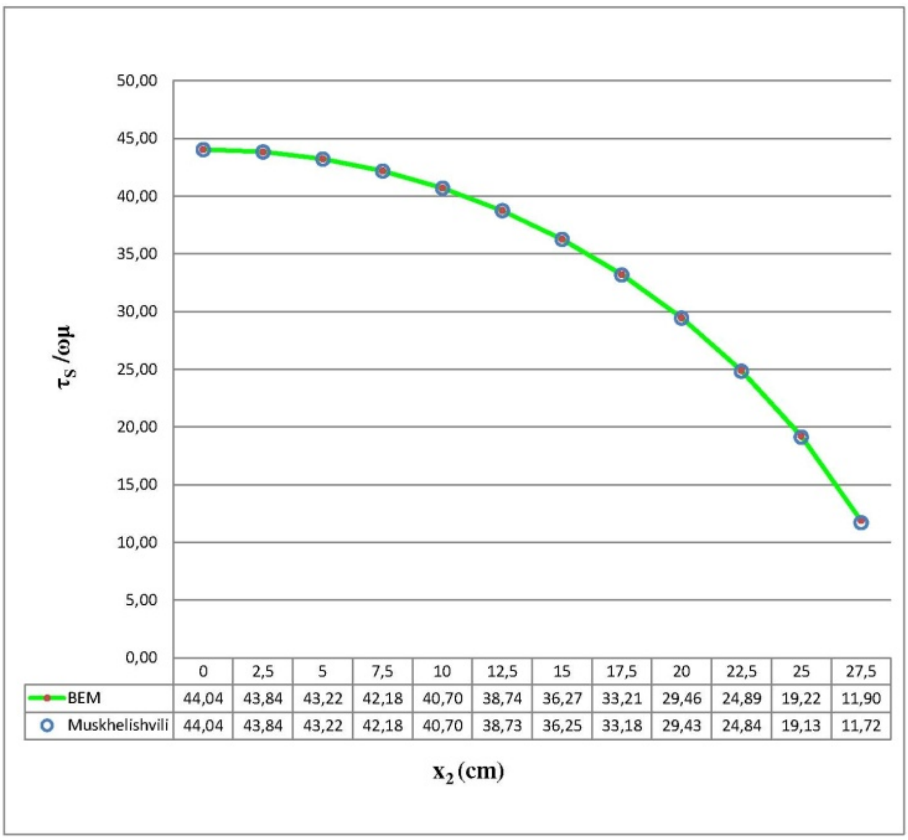

Figure 12. Variation of $\tau_S/\omega\mu$ versus x_2 on BC line in rectangular

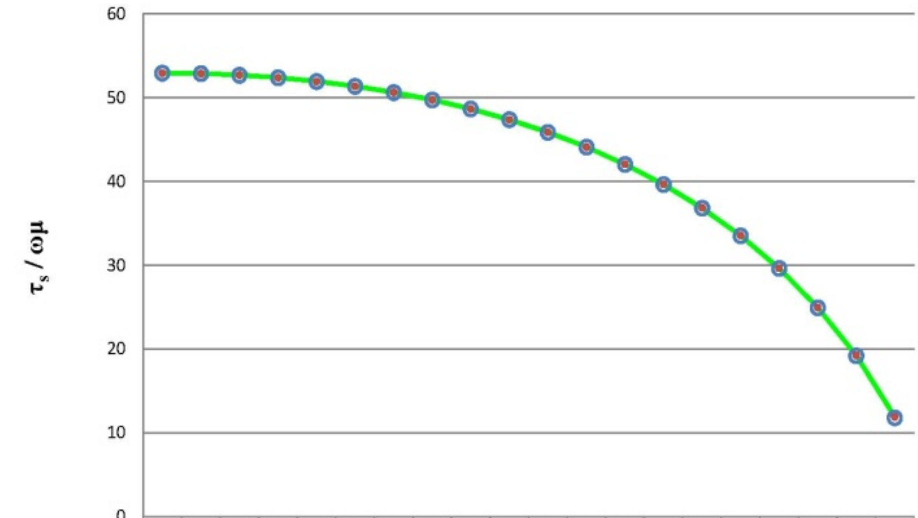

x_1 (cm)	0	2,5	5	7,5	10	12,5	15	17,5	20	22,5	25	27,5	30	32,5	35	37,5	40	42,5	45	47,5
BEM	52,94	52,88	52,7	52,39	51,95	51,37	50,63	49,74	48,66	47,39	45,88	44,12	42,06	39,65	36,84	33,54	29,63	24,96	19,24	11,91
Muskhelishvili	52,94	52,88	52,69	52,38	51,94	51,36	50,63	49,73	48,66	47,38	45,87	44,11	42,05	39,64	36,82	33,52	29,61	24,93	19,19	11,8

x_1 (cm)

Figure 13. Variation of $\tau_S/\omega\mu$ versus x_1 on EC line in rectangular

In the first problem there were two symmetry axes but in the second there is only one as x_2. For the second problem variation of φ function on ABCDEF boundary are given in Figure 14, Figure 15 and Figure 16. The variation of τ_{23} versus x_1 on GA given in Figure 17. The variations of τ_{13} and τ_{23} versus x_2 on DK line are given in Figure 18 and Figure 19 respectively. For this cross-section R has been found as 4497964,92554 cm^4. Variation relative to full rectangular is very small for this quantity. Variations of $\tau_s/(\mu\omega)$ on ABCDEF boundary are given in Figure 20, Figure 21 and Figure 22.

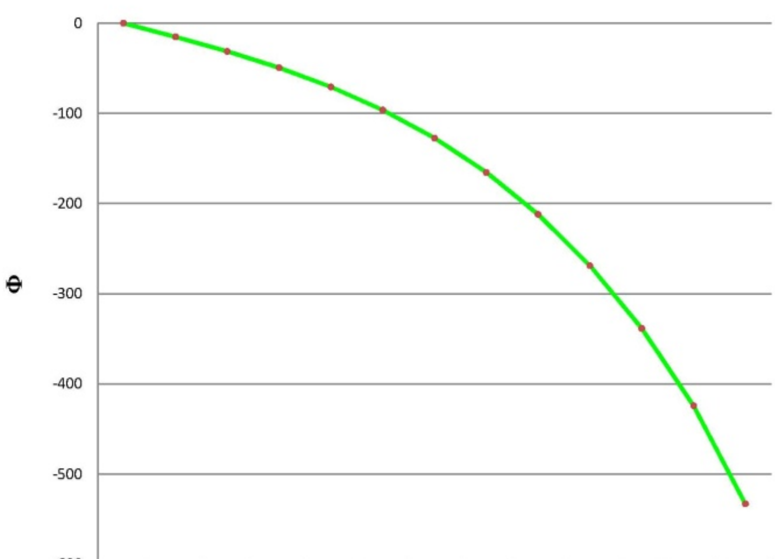

x_2 (cm)	0	2,5	5	7,5	10	12,5	15	17,5	20	22,5	25	27,5	30
BEM	0	-15,08	-31,18	-49,35	-70,67	-96,28	-127,4	-165,5	-212	-268,8	-338,5	-424,1	-533,1

x_2 (cm)

Figure 14. Variation of φ versus x_2 on AB line in rectangular with a notch

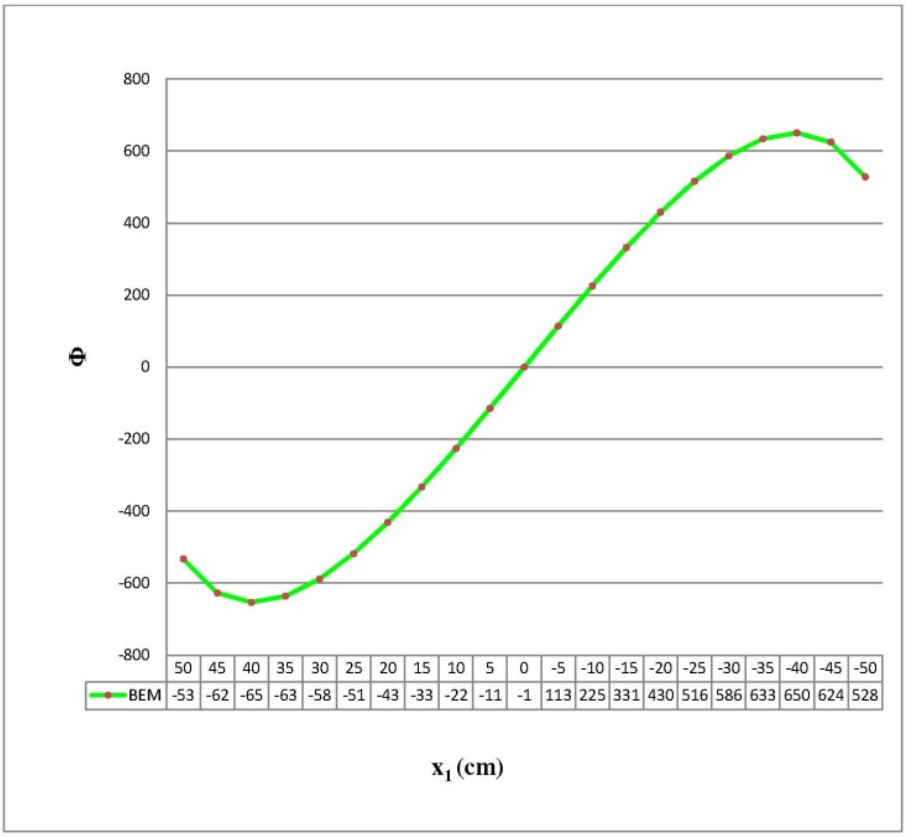

Figure 15. Variation of φ versus x_1 on BE line in rectangular with a notch

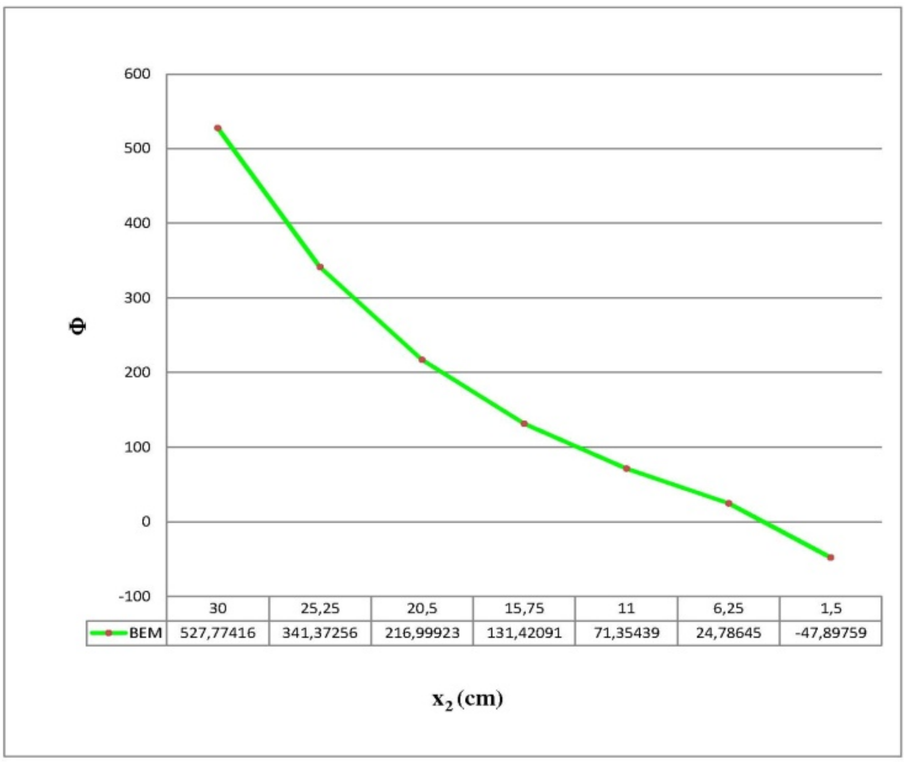

Figure 16. Variation of φ versus x_2 on EF line in rectangular with a notch

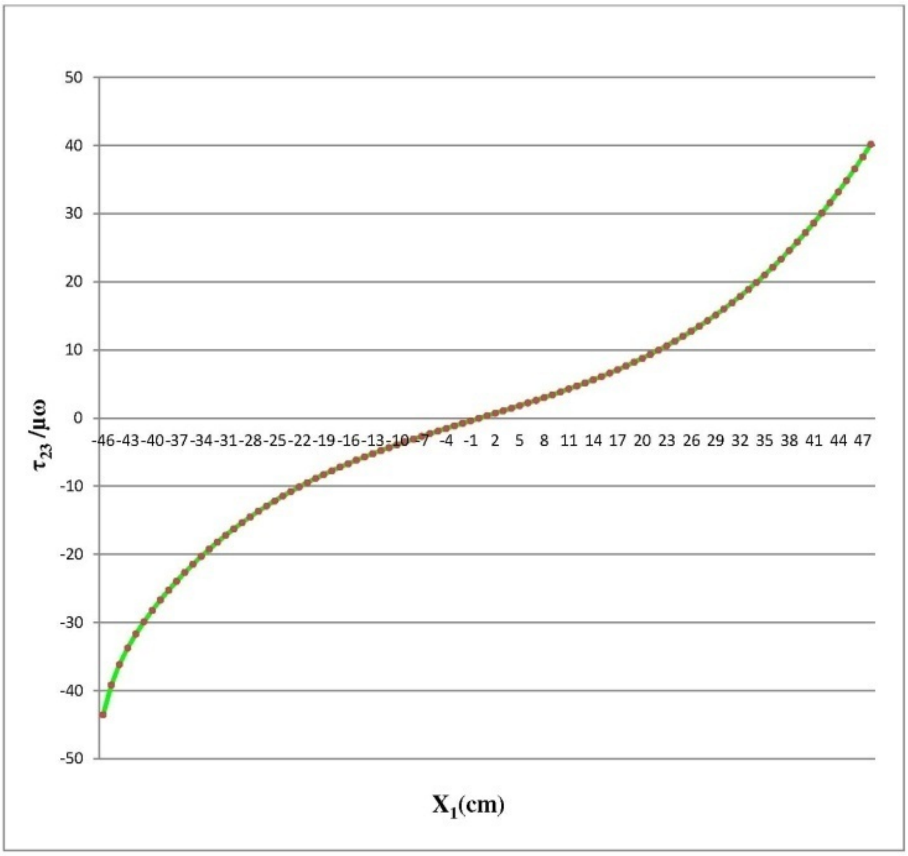

Figure 17. Variation of $\tau_{23}/\omega\mu$ versus x_1 on GA line in rectangular with a notch

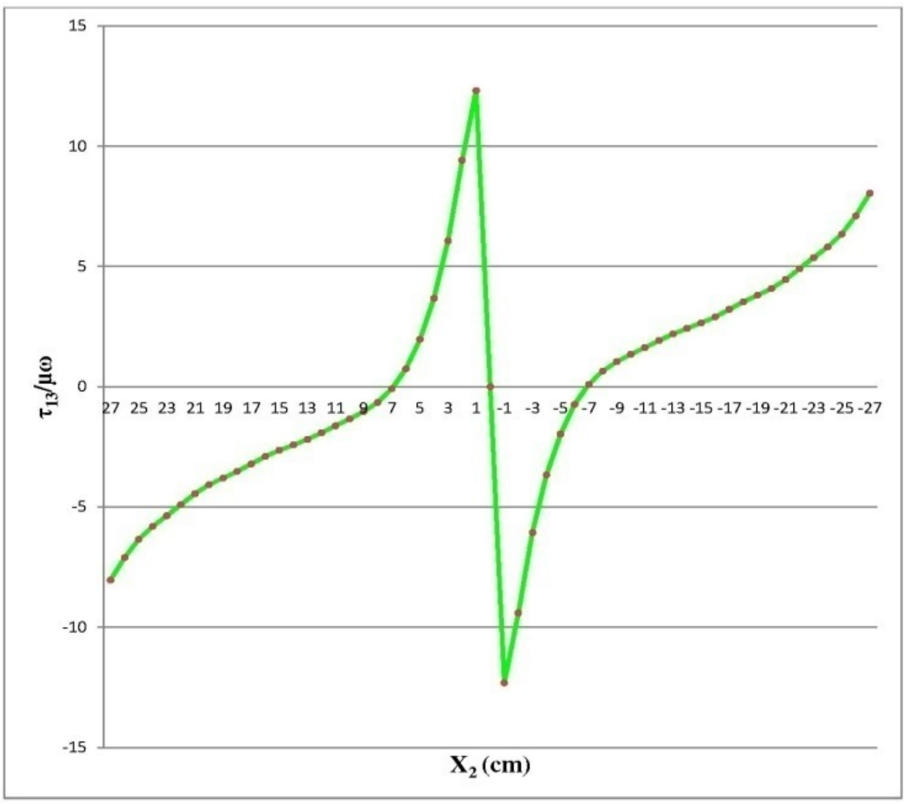

Figure 18. Variation of $\tau_{13}/\omega\mu$ versus x_2 on DK line in rectangular with a notch

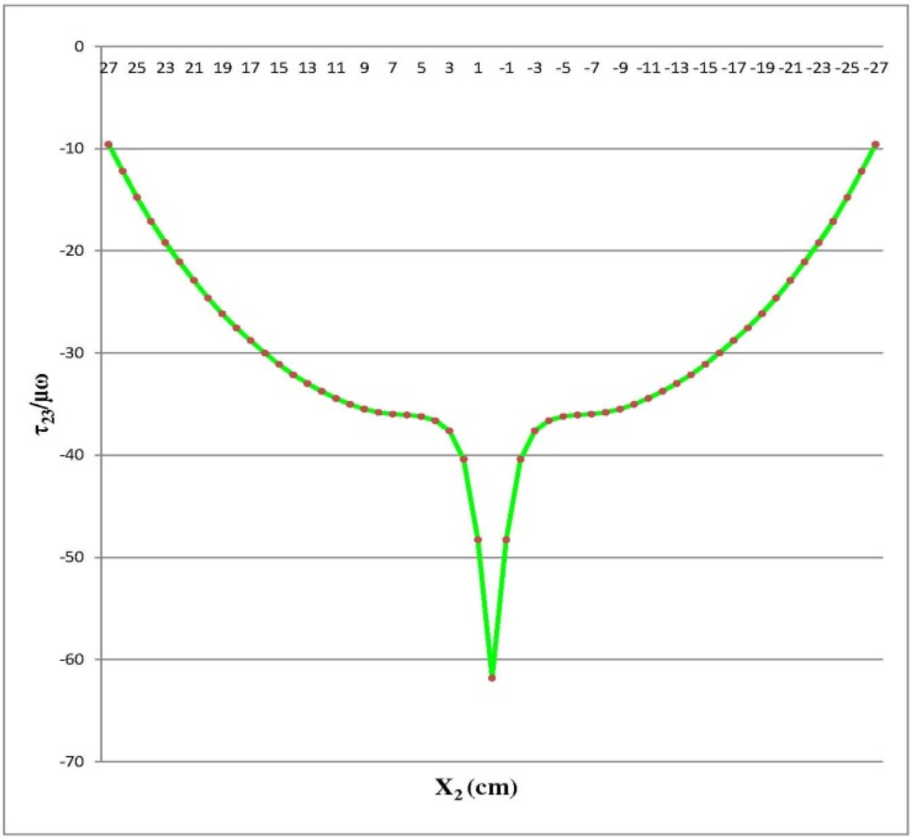

Figure 19. Variation of $\tau_{23}/\omega\mu$ versus x_2 on DK line in rectangular with a notch

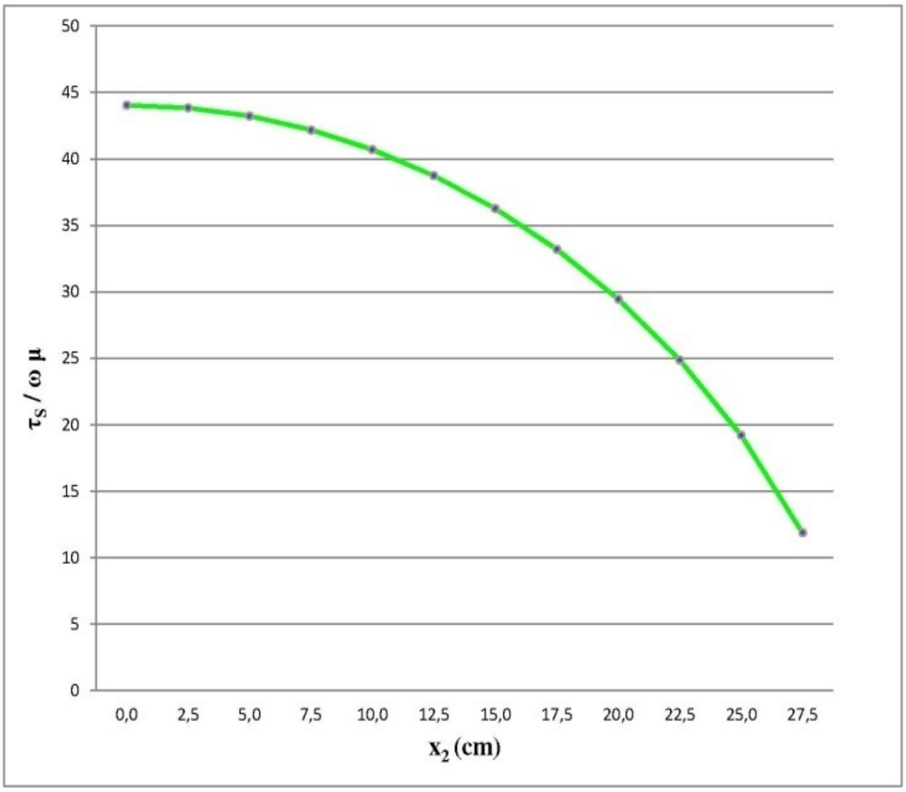

Figure 20. Variation of $\tau_S/\omega\mu$ versus x_2 on AB line in rectangular with a notch

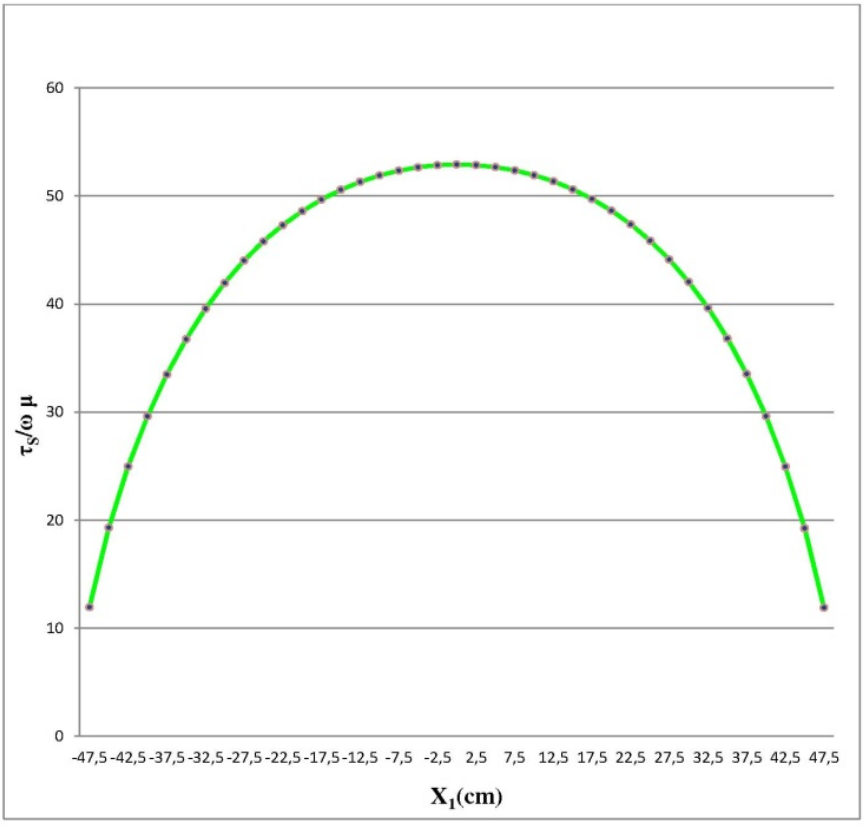

Figure 21. Variation of $\tau_S/\omega\mu$ versus x_1 on EB line in rectangular with a notch

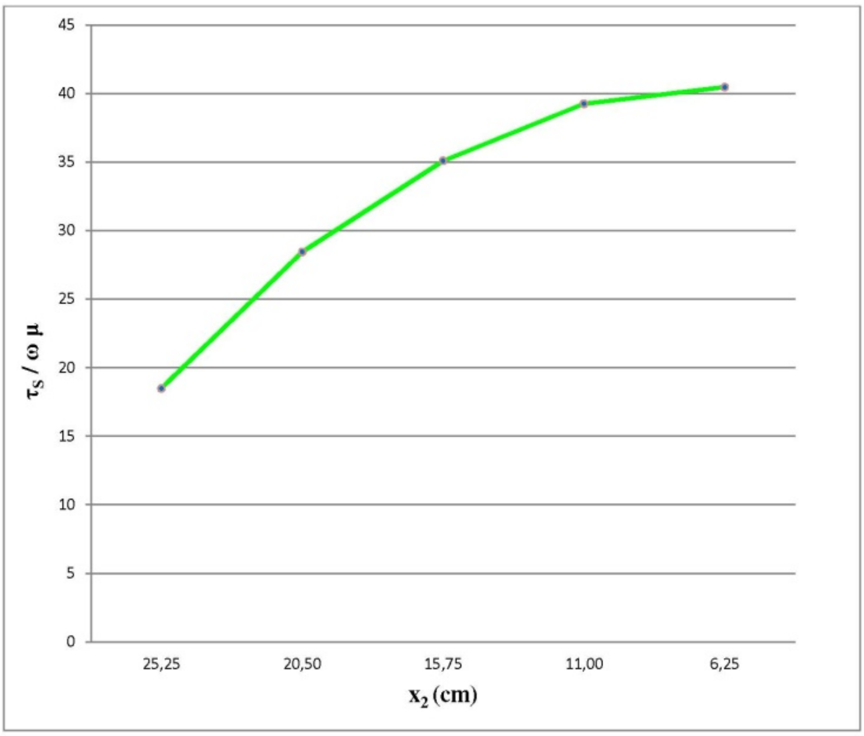

Figure 22. Variation of $\tau_S/\omega\mu$ versus x_2 on EF line in rectangular with a notch

4. Third Sample Problem

This problem is an extension of the proposed method to problems having multiple connected cross-sections and different materials. The selected problem is a rectangular concrete column with four rebars. The ratio of shear modules of concrete and iron is ½. (e.g Figure 23)

This problem can be thought as the summation of two different problems. First problem is a rectangular cross-section with four holes. These holes are symmetric relative to x_1 and x_2 axes. For this domain boundary is the summation of external boundary of the rectangular and the boundaries of the holes. And the equation (25) takes the following form for this problem

$$\begin{matrix} \varphi(y) & (y \in S_1) \\ 0 & (y \notin S_1) \end{matrix} =$$

$$\oint_{C_S} \frac{1}{2\pi}\phi(x_1, x_2)\left[\frac{(x_1-y_1)n_1-(x_2-y_2)n_2}{\rho^2}\right]dC$$

$$-\frac{1}{2\pi}\int_{C_S}\left(x_2 n_1 \ln\rho - x_1 n_2 \ln\rho\right)dC$$

$$-\frac{1}{2\pi}\int_{C_1+C_2+C_3+C_4}\left(\frac{t_3}{\mu_1\omega}\ln\rho\right)dC \qquad (65)$$

Here C_S represents the whole boundary. C_i (i=1,2,3,4) represents the boundary of the i' th hole and $t_3/\mu_1\omega$ represents the third component of the surface traction vector on any surface hole. The assumptions and definitions up to now are valid for this problem too. It is assumed that the new unknown $t_3/\mu_1\omega$ is also linear on the linear elements defined on holes. But number of the unknowns is more than number of the equations. Then a single rebar must also be considered. The φ values are the same at the corresponding points of the hole and the rebar. But there is also t_3 component of the surface traction vector on the rebar and this term involves $\mu_2\omega$ divisor instead of $\mu_1\omega$. And the sign of it opposite for the corresponding points with the hole. Considering these facts and applying the method explained before the unknowns of this problem can also be solved. Unknowns are the φ values on the whole boundary and in addition to these the third component of the surface traction vector on the boundaries of the holes. After construction of necessary linear equations this unknowns can be solved. For the selected example results are plotted in Figure 24, Figure 25, Figure 26 and Figure 27. After these the variations of $\tau_{13}/\mu_1\omega$ and $\tau_{23}/\mu_1\omega$ functions are plotted one vertical and one horizontal line in Figure 28, Figure 29, Figure 30 and Figure 31.

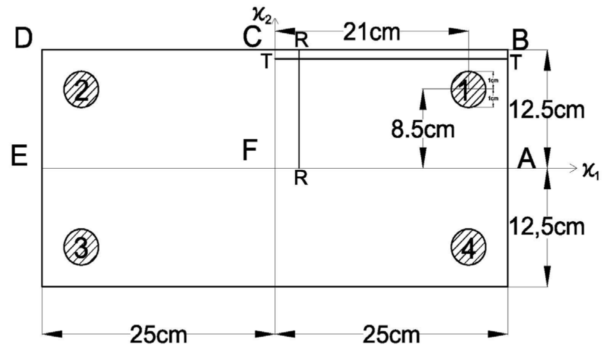

Figure 23. Reinforced rectangular concrete column

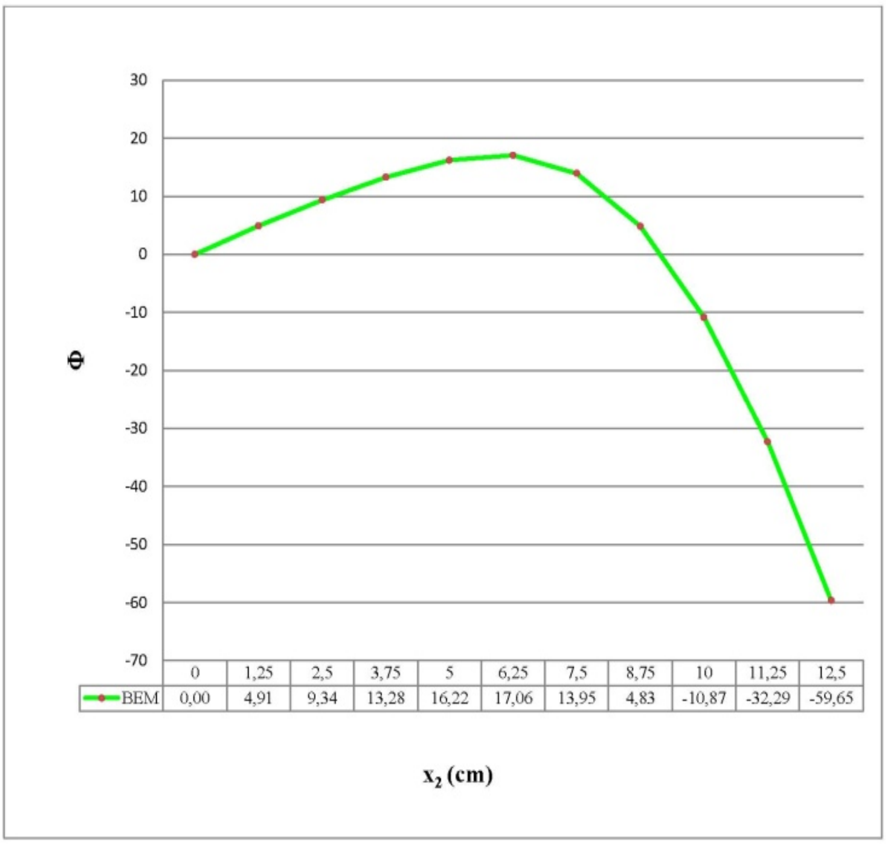

Figure 24. Variation of φ versus x_2 on AB line in Figure 23

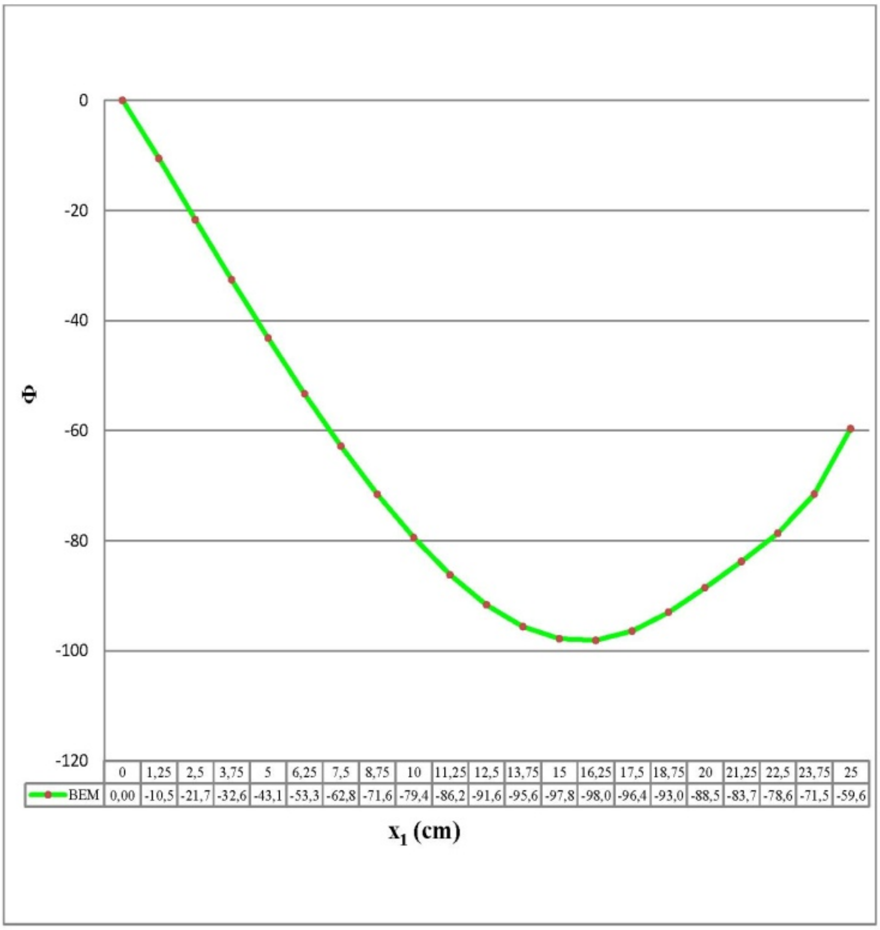

Figure 25. Variation of φ versus x_2 on CB line in Figure 23

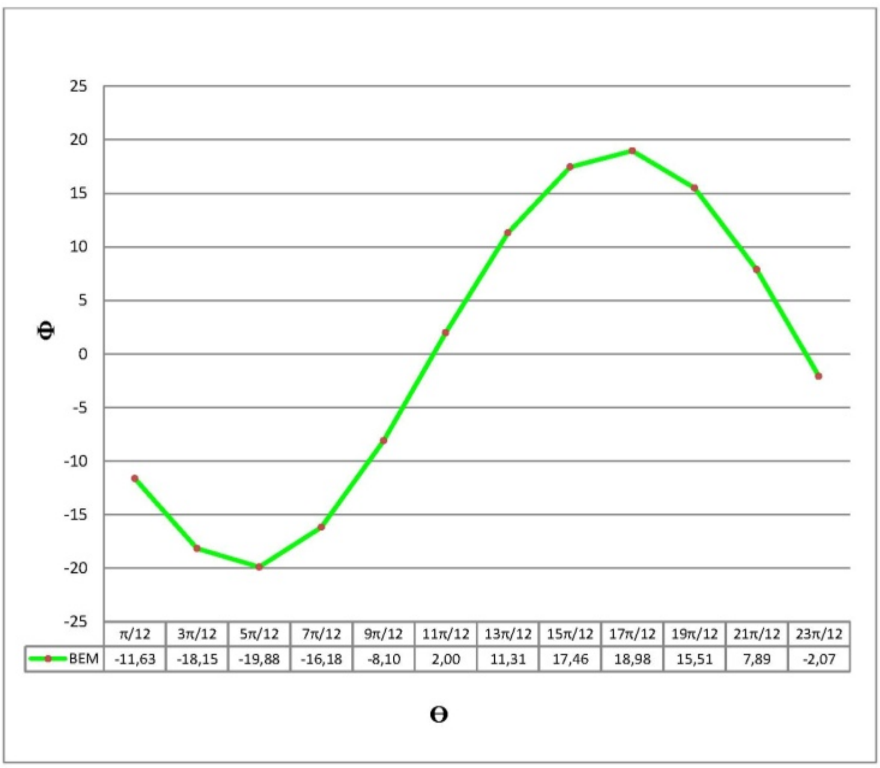

Figure 26. Variation of φ versus Θ on the boundary of the first hole

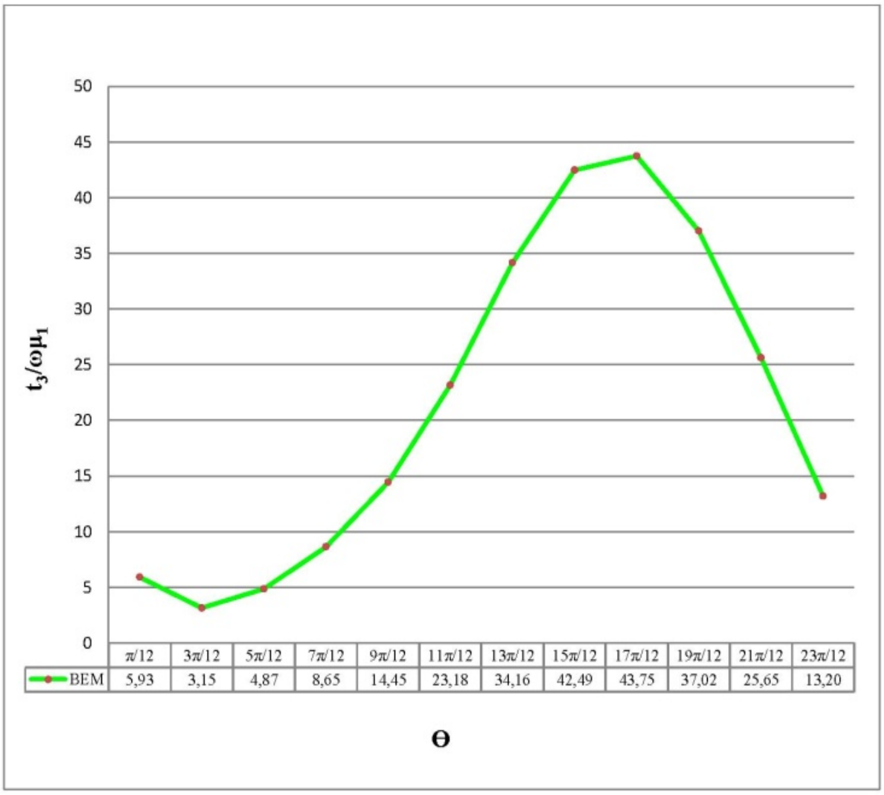

Figure 27. Variation of $t_3/\omega\mu_1$ versus Θ on the boundary of the first hole

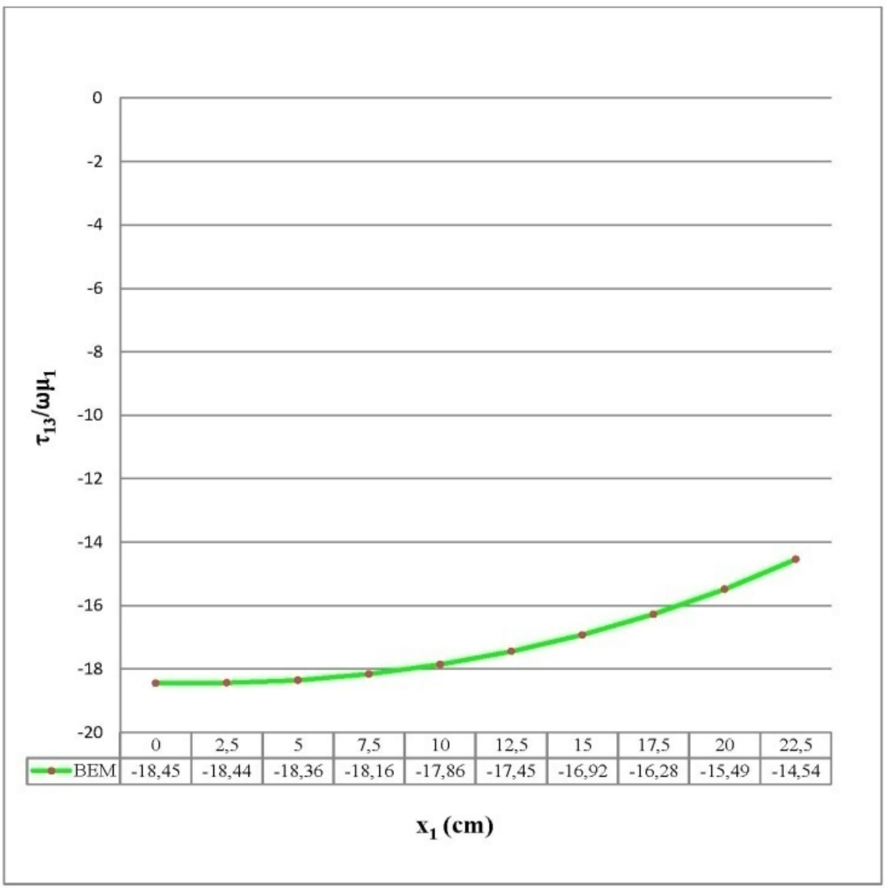

Figure 28. Variation of $\tau_{13}/\omega\mu_1$ versus x_1 on x_2=11cm line

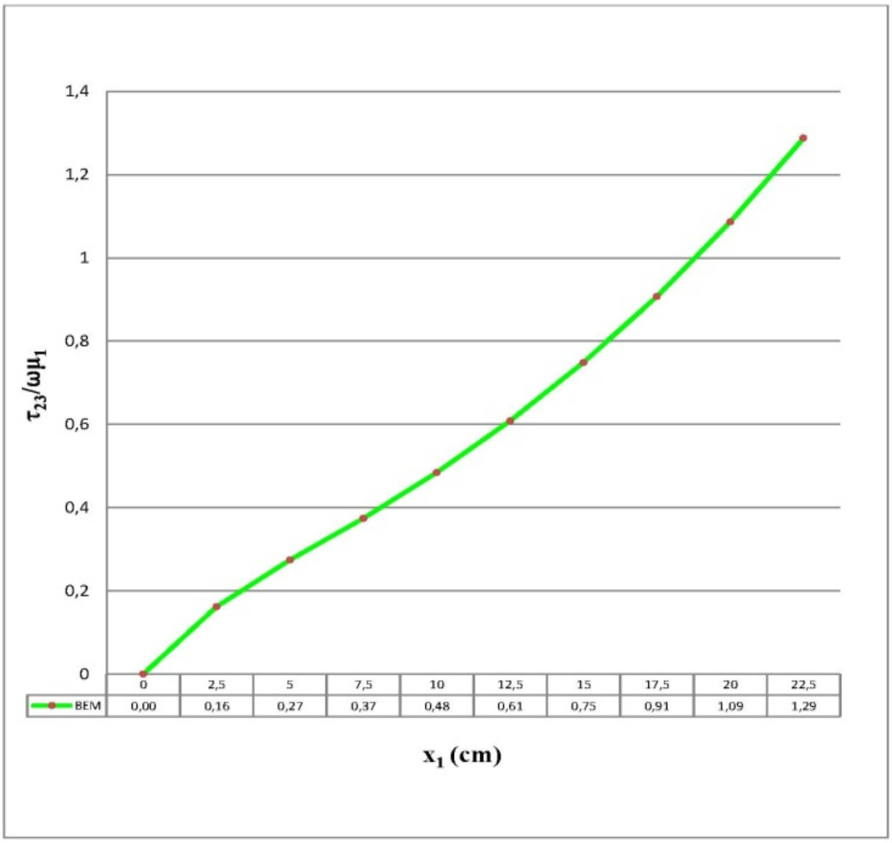

Figure 29. Variation of $\tau_{23}/\omega\mu_1$ versus x_1 on x_2=11cm line

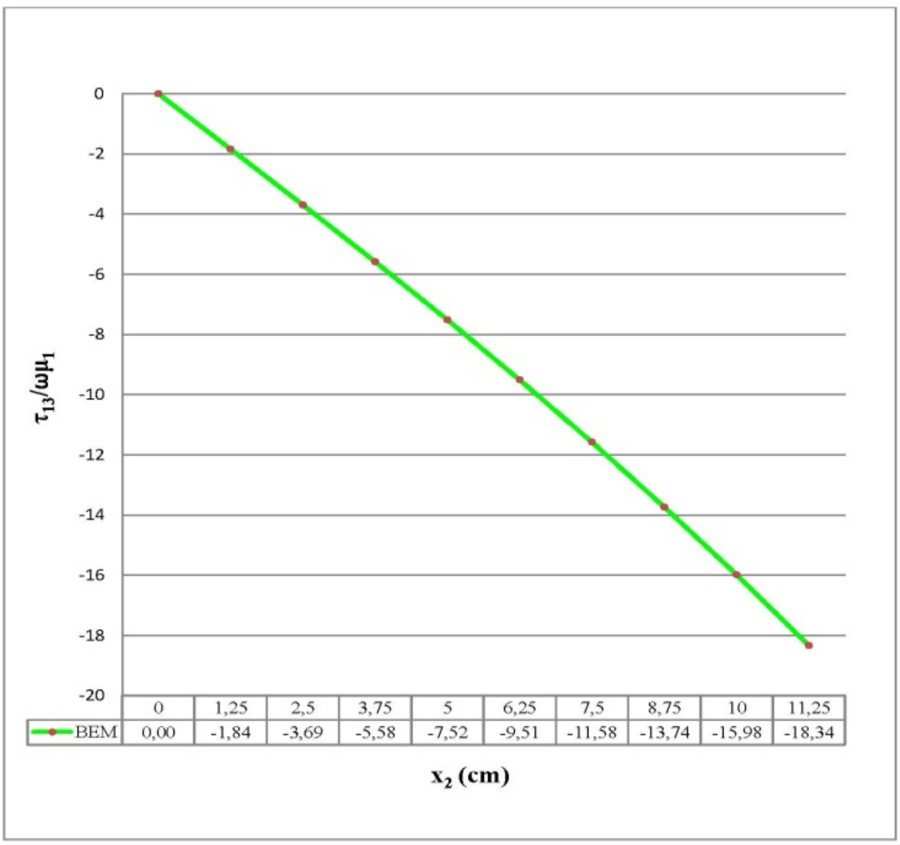

Figure 30. Variation of $\tau_{13}/\omega\mu_1$ versus x_2 on x_1=5cm line

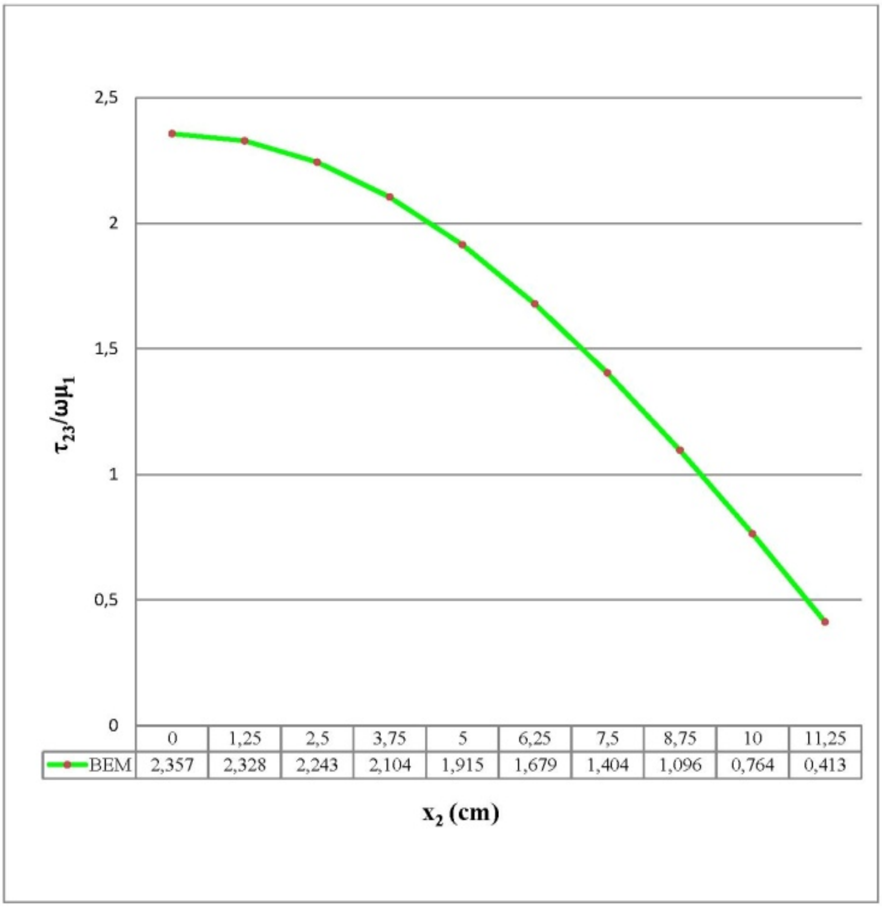

x_2 (cm)	0	1,25	2,5	3,75	5	6,25	7,5	8,75	10	11,25
BEM	2,357	2,328	2,243	2,104	1,915	1,679	1,404	1,096	0,764	0,413

Figure 31. Variation of $\tau_{23}/\omega\mu_1$ versus x_2 on x_1=5 cm line

5. Conclusions

A boundary element formulation is developed for torsion problems in bars with arbitrary cross-sections. At first this formulation is valid for only cross-sections with simple-connected contours. But formulation of the problem can be extended to multiple-connected cross-sections since it is given as a stress problem of elasticity. Besides mixed-boundary problems can also be solved extending the formulation. Formulation involves the calculation of displacement components inside and the boundary of the cross-section. For the calculation of stresses two different formulations are given. The first one is for the stress components inside the cross-section while the second is for the unknown stress component on the boundary. But formulation allows calculating the unknown stress component only at the boundary points with a single tangent. First selected sample problem is a rectangular. The results are compatible with the results of analytical solution of this problem given by Muskhelishvili. The relative error is practically zero for displacements and stresses. But this value is 9/10000 for determination of torsional rigidity. Second sample problem is also a rectangular with a triangular notch. For this problem it is understood that at the points far from the notch whole quantities are very near with those belong to the full rectangular. Besides the variation of torsional rigidity is very small because of the small notch. All singularities arising in boundary element formulation have been eliminated. The biggest differences occur near the tip of the notch. At the tip u_3 displacement has been calculated but at this point unknown stress component cannot be calculated. However one can approach to this point from inside of the region. For this purpose the variations of $\tau_{13}/\mu\omega$ and $\tau_{23}/\mu\omega$ shear stresses, versus x_2 have been plotted in Figures 18-19 on a line which is parallel to x_2 axis and .5 cm to the tip of the notch. At the point N (e.g. Figure 5) $\tau_{13}/\mu\omega$ =0 $\tau_{23}/\mu\omega$ =-61,8262 cm have been found. For full rectangular same quantity is $\tau_{23}/\mu\omega$ =-39,2292 cm. Magnification factor is nearly 1,58. For the selected third sample problem method is extended to multiple-connected regions and also selected problem involves two different materials. For a full rectangular R has been found to be 178864,77cm^4 and but for reinforced column same value has been found as 354738,25cm^4. The most interesting result of this problem is that φ function change sign in one quarter.

Appendix

$$W1(I,J)=\frac{1}{2\pi}\left[\tan^{-1}\frac{x_2(J+1)-x_2(I)}{x_1(J+1)-x_1(I)}-\tan^{-1}\frac{x_2(J)-x_2(I)}{x_1(J)-x_1(I)}\right]$$

$$T(I,J) =$$

$$\frac{1}{2\pi}\Big[\big[(x_1(J)-x_1(I))n_1(J)+(x_2(J)-x_2(I))n_2(J)\big]$$

$$\left[\ln\frac{\sqrt{(x_1(J+1)-x_1(I))^2+(x_2(J+1)-x_2(I))^2}}{\sqrt{(x_1(J)-x_1(I))^2+(x_2(J)-x_2(I))^2}}\right]$$

$$\big[n_2(J)(x_1(J)-x_1(I))-n_1(J)(x_2(J)-x_2(I))\big]$$

$$\left[\tan^{-1}\frac{x_2(J+1)-x_2(I)}{x_1(J+1)-x_1(I)}-\tan^{-1}\frac{x_2(J)-x_2(I)}{x_1(J)-x_1(I)}\right]\Big]$$

$$W2(I,J)=\frac{1}{2\pi}\Bigg[-\frac{\rho_B^2}{2}\ln\rho_B+\frac{\rho_A^2}{2}\ln\rho_A+\frac{\rho_B^2}{2}-\frac{\rho_A^2}{2}$$

$$+(y_1 n_2(J)-y_2 n_1(J))\big[\ln\rho_B(l(J)+n_1(J)(x_{A2}-y_2)$$

$$-n_2(J)(x_{A1}-y_1))-l(J)+\big[n_1(J)(x_{A1}-y_1)+n_2(J)$$

$$(x_{A2}-y_2)\big](\arctan\frac{x_{B2}-y_2}{x_{B1}-y_1}-\arctan\frac{x_{A2}-y_2}{x_{B2}-y_2}\Big]\Bigg]$$

Here

$\rho_A = |x(J-1)-x(I)|$ $\qquad \rho_B = |x(J)-x(I)|$

$x_{A1} = x_1(J-1)$ $\qquad x_{B1} = x_1(J)$

$y_1 = x_1(I)$ $\qquad y_1 = x_1(I)$

$x_{A2} = x_2(J-1)$ $\qquad x_{B2} = x_2(J)$

REFERENCES

[1] Muskhelishvili N.I., Some “Basic Problems of The Mathematical Theory of Elasticity”, 1963.

[2] Ely J. F. and Zienkiewicz O. C., “Torsion of compound bars - a relaxation solution”, International Journal of Mechancial Sciences, vol 1, pp. 356-365. 1960.

[3] Jaswan M. A. and Ponter A. R. S., 1963: An integral equation solution of the inhomogeneous torsion problem, Proc. Roy Soc. A, Vol 273, pp. 237-246. 1963.

[4] Katsikadelis J.T. and Sapountzakis E. J. “Torsional of composite bars by boundary element method”, Journal of Engineering Mechanics Vol. 111, No:9, 1985.

[5] Banerjee P.K. and Butterfield R., (1981) Boundary element methods in engineering science.

[6] Kadioglu N, Ataoglu S, "A BEM implementation for 2D problems in plane orthotropic elasticity", Structural Engineering and Mechanics, Vol. 26, No. 5, 07/2007, pp. 591-615, ISSN:1225-4568, Techno-Press, http://technopress.kaist.ac.kr/.